Bubble and droplet motion in binary mixtures:
Evaporation-condensation mechanism and Marangoni effect

Akira Onuki

Department of Physics, Kyoto University, Kyoto 606-8502, Japan
(Dated: March 19, 2009)

Bubble and droplet motion in binary mixtures is studied in weak heat and diffusion fluxes and in gravity by solving the linearized hydrodynamic equations supplemented with appropriate surface boundary conditions. Without gravity, the velocity field is induced by evaporation and condensation at the interface and by the Marangoni effect due to a surface tension gradient. In pure fluids, the latter nearly vanishes since the interface temperature tends to the coexistence temperature $T_{\rm cx}(p)$ even in heat flow. In binary mixtures, the velocity field can be much enhanced by the Marangoni effect above a crossover concentration c^* inversely proportional to the radius R of the bubble or droplet. Here c^* is usually very small for large R for non-azeotropic mixtures. The temperature and concentration deviations are also calculated.

I. INTRODUCTION

On earth, bubble motion in liquid is caused by gravity. Buoyancy effects increase dramatically with increasing the droplet radius R. Due to the viscosity of liquid, it moves at a constant velocity v_g estimated as [1, 2, 3]

$$v_g \sim \frac{\rho - \rho'}{\eta} R^2 g, \qquad (1.1)$$

where g is the gravity acceleration. Hereafter ρ and η (ρ' and η') are the mass density and the shear viscosity outside (inside) the bubble. Another method of inducing bubble motion is to apply a heat flux Q. It is well-known that a surface tension variation on the surface gives rise to a Marangoni velocity field [1], causing bubble motion to lower the surface free energy. Neglecting phase transition, Young *et al.* [4] calculated it as

$$v_Y \sim \frac{\gamma_1}{\eta \lambda} RQ, \qquad (1.2)$$

where λ is the thermal conductivity in liquid. The surface tension variation $\delta \gamma$ is assumed to be given by

$$\delta \gamma = -\gamma_1 \delta T, \qquad (1.3)$$

where δT is the ambient temperature deviation, so $v_Y \sim \delta\gamma/\eta$. Here $\gamma_1 > 0$ for most fluids, but $\gamma_1 < 0$ for some fluid mixtures. If a liquid is heated from a boundary at zero gravity, a suspended bubble is attracted to the warmer boundary for $\gamma_1 > 0$ with a velocity of order $-v_Y$, until it is attached to the wall. In heat flux on earth, the gravity and Marangoni mechanisms can compete. We mention an experiment of applying heat flow from below to silicone oil containing air bubbles, where temperature gradients of order $10\text{-}10^2$ K/cm balanced with the buoyancy and held the bubbles stationary [4]. Subsequent microgravity experiments on the Marangoni effect have been performed without phase change [5, 6].

However, first order phase transition between gas and liquid (evaporation and condensation) should take place on the bubble surface. This is particularly the case for pure (one-component) fluids, where the pressure p is nearly homogeneous outside the bubble for slow motions and the interface temperature should then be close to the coexistence temperature $T = T_{\rm cx}(p)$ at given p even in heat flux. Thus, in pure fluids, the temperature gradient should nearly vanish inside bubbles without Marangoni flow. Recently such temperature profiles have been calculated from linearized hydrodynamic equations supplemented with appropriate surface conditions [7] and numerically in the dynamic van der Waals theory [8]. Balance of a heat flux due to latent heat convection and an applied heat flux Q gives the amplitude of the convective velocity inside the bubble as

$$v_c \sim \frac{Q}{\rho' T \Delta s}, \qquad (1.4)$$

where $\Delta s = s' - s$ is the entropy difference per unit mass. If a bubble (droplet) is suspended in liquid (gas) at zero gravity, it migrates toward a warmer (cooler) boundary with a velocity of order v_c [8]. In this evaporation-condensation mechanism, a bubble in liquid is attracted to a warmer boundary wall, which is consistent with experiments on pure fluids without gravity [9].

In this paper, we investigate bubble and droplet motion in binary mixtures, where the Marangoni effect and the evaporation-condensation can be both important. In analyzing boiling experiments, Marek and Straub [10] argued that convection around a bubble should be dominantly caused by the Marangoni effect due to a very small amount of a noncondensable gas. If a surfactant is added as a solute, such a contamination effect should be even more enhanced [1, 11]. In our theory we shall see that the Marangoni velocity for dilute non-azeotropic binary mixtures is of order,

$$v_M \sim \frac{\gamma_1}{k_B n D_0 \eta} cRQ, \qquad (1.5)$$

where n is the number density, D_0 is the solute diffusion constant in liquid, and k_B is the Boltzmann constant.

Balance of v_c and v_M yields a crossover concentration c^* given by

$$c^* = a_1/R, \qquad (1.6)$$

where $a_1 = (k_B D_0 \eta/T)(n/\rho' \Delta s |\gamma_1|)$ is usually a microscopic length far from the critical point. See sentences below Eq.(4.16) for a_1 near the critical point. Unless γ_1 is very small, c^* is very small for large droplet radius $R \gg a_1$. For $c \gg c^*$ the hydrodynamic motion is mostly due to the Marangoni effect.

Furthermore, there seems to have been no fundamental argument on the coefficient γ_1 in Eq.(1.3) in binary mixtures in nonequilibrium. In this paper we assume the continuity of the temperature and the chemical potentials and neglect the pressure deviations at the interface. Then it follows $\gamma_1 = -(\partial \gamma/\partial T)_{cx,p}$, where the derivative is along the isobaric line on the coexistence surface. This γ_1 tends to a well-defined limit in the dilute limit of binary mixtures ($c \to 0$). Recently, it has been calculated for nonelectrolyte binary mixtures [12]. Particularly near the solvent criticality, its mean-field expression at small solute concentration reads

$$\gamma_1 = -\frac{d\gamma_0}{dT}\frac{dp_c}{dX}\frac{1}{K_{\mathrm{Kr}}}, \qquad (1.7)$$

where $\gamma_0(T)$ is the surface tension of the pure solvent, $p_c(X)$ is the critical pressure dependent on the solute molar fraction X on the critical line, and K_{Kr} is the so-called Krichevskii parameter (having the dimension of pressure) [13, 14, 15, 16, 17]. See Appendix C for discussions of K_{Kr}. While $d\gamma_0/dT < 0$ for pure fluids, the two parameters dp_c/dX and K_{Kr} can be both positive and negative, depending on the solute molecular size and the solute-solvent interaction. For example, if near-critical CO_2 is a solvent, use of data in Ref.[17] gives the value of $(dp_c/dX)/K_{\mathrm{Kr}}$ in Eq.(1.7) for various solutes, which is 0.90 for neon but is -0.81 for pentanol [12].

In their experiment, Vochten and Petre [18] found that the surface tension between air and aqueous mixtures containing high carbon alcohols more than 1mM exhibits a minimum as a function of the temperature at constant pressure and molar fraction. In such fluids, $\gamma_1 < 0$ at temperatures higher than that giving the minimum. Inspired by their finding, consequences of negative γ_1 have been discussed in two-phase hydrodynamics particularly to develop heat pipes for utilization in space [19, 20, 21, 22, 23]. Remarkably, if the sign of γ_1 is changed, the direction of the Marangoni flow is reversed. As a result, if $\gamma_1 < 0$, bubbles are easily detached from the heater in boiling. This leads to a liquid inflow onto the heater suppressing its dryout, so fluid mixtures with $\gamma_1 < 0$ have been called self-rewetting fluids. On earth, Abe [21] observed a considerable decrease in the size of rising bubbles with addition of 1-butanol (6 wt%) to water (where $\gamma_1 < 0$). Adding 1-heptanol (0.1 wt%) to water, Savino *et al.* [23] observed bubble motion toward a cooler end in a horizontal glass tube.

This paper will present linear analysis in the simplest case of a spherical bubble or droplet in binary mixtures in weak heat and diffusion fluxes and in gravity. In Section II, we will give linear hydrodynamic equations and surface boundary conditions including the Marangoni condition for the tangential stress [1, 24]. In Section III, we will solve the equations in steady states in the axisymmetric geometry. In Section IV, we will examine the consequences in dilute mixtures. Estimations near the critical point will also be presented. In Section V, the velocity field around a bubble or droplet will be displayed in various cases.

II. BASIC EQUATIONS

A. Spherical droplet

We place a gas bubble in liquid with radius R in a non-electrolyte binary fluid mixture. We do not assume surface adsorption due to the amphiphilic interaction. The following results can be used also for the case of a liquid droplet in gas by exchanging "liquid" and "gas". Suppose an equilibrium state in the gravity-free condition (see Appendix A of Ref.[7]), where the temperature T and the chemical potentials of the two components μ_1 and μ_2 are homogeneous. The pressure p is a constant p_0 in the exterior $r > R$ and is $p_0 + 2\gamma/R$ in the interior $r < R$ (from the Laplace law, where γ is the surface tension and r is the distance from the bubble center. The interior and exterior concentrations are determined from the thermodynamics of binary mixtures [12].

We then apply weak heat and diffusion fluxes and a gravity acceleration g. They are all along the z axis taken to be in the upward vertical direction $\parallel \boldsymbol{e}_z$. Hereafter $\boldsymbol{e}_z$ denotes the unit vector along the z axis. The gradients of the temperature T and the mass fraction c are homogeneous far from the bubble and are written as

$$\mathcal{T} = \left(\frac{dT}{dz}\right)_{r=\infty}, \quad \mathcal{C} = \left(\frac{dc}{dz}\right)_{r=\infty}. \qquad (2.1)$$

It is convenient to introduce the chemical potential difference per unit mass as

$$\mu = \mu_2 - \mu_1, \qquad (2.2)$$

which has a gradient given by

$$\mathcal{M} = \left(\frac{d\mu}{dz}\right)_{r=\infty} = \left(\frac{\partial \mu}{\partial T}\right)_{pc}\mathcal{T} + \left(\frac{\partial \mu}{\partial c}\right)_{pT}\mathcal{C}, \qquad (2.3)$$

Here the thermodynamic derivatives are taken in the outer phase in the isobaric condition.

The hydrodynamic equations are linearized with respect to $\mathcal{T}$, $\mathcal{C}$, and g. The deviations are all proportional to one of these quantities. After a transient relaxation, the bubble moves at a constant velocity v_D in the vertical z axis. We may then take the origin of the reference frame

at the bubble center and seek a steady axisymmetric solution of the hydrodynamic equations with appropriate boundary conditions. To linear order in $\mathcal{T}$, $\mathcal{C}$, and g, the bubble shape is spherical, as assumed in the previous theories [2, 3, 4]. Deviation from sphericity occurs from second orders in these quantities.

In the following calculation it is convenient to use the spherical coordinates (r, θ, φ) with the origin at the bubble center. Using the solid angles θ and φ we define the three orthogonal unit vectors,

$$
\begin{aligned}
\boldsymbol{e}_1 &= r^{-1}\boldsymbol{r} = (\sin\theta\cos\varphi, \sin\theta\sin\varphi, \cos\theta), \\
\boldsymbol{e}_2 &= \frac{\partial}{\partial\theta}\boldsymbol{e}_1 = (\cos\theta\cos\varphi, \cos\theta\sin\varphi, -\sin\theta), \\
\boldsymbol{e}_3 &= \boldsymbol{e}_1 \times \boldsymbol{e}_2 = (-\sin\varphi, \cos\varphi, 0). \quad (2.4)
\end{aligned}
$$

The interface normal is along $\boldsymbol{e}_1$. The velocity field $\boldsymbol{v}$ around the bubble will be assumed to be orthogonal to $\boldsymbol{e}_3$ or $\boldsymbol{e}_3 \cdot \boldsymbol{v} = 0$.

B. Hydrodynamic equations

The mass densities of the two components are written as ρ_1 and ρ_2. The total mass density ρ and the mass fraction c of the second component are defined by

$$
\rho = \rho_1 + \rho_2, \quad c = \rho_2/\rho. \quad (2.5)
$$

The mass fluxes of the two components are $\rho_1\boldsymbol{v} - \boldsymbol{I}$ and $\rho_2\boldsymbol{v} + \boldsymbol{I}$, where $\boldsymbol{v}$ is the velocity field and $\boldsymbol{I}$ is the diffusive flux. The continuity equations for ρ and ρ_1 are [25]

$$
\frac{\partial}{\partial t}\rho = -\nabla \cdot (\rho\boldsymbol{v}), \quad (2.6)
$$

$$
\frac{\partial}{\partial t}(\rho c) = -\nabla \cdot (\rho c\boldsymbol{v} + \boldsymbol{I}). \quad (2.7)
$$

We express $\boldsymbol{I}$ in terms of the isothermal mutual diffusion constant D and the thermal diffusion ration k_T as [25]

$$
\boldsymbol{I} = -\rho D(\nabla c + T^{-1}k_T\nabla T). \quad (2.8)
$$

The momentum density $\rho\boldsymbol{v}$ obeys

$$
\frac{\partial}{\partial t}\rho\boldsymbol{v} + \nabla \cdot (\rho\boldsymbol{v}\boldsymbol{v}) = -\nabla p + \nabla \cdot \overleftrightarrow{\sigma} - \rho g\boldsymbol{e}_z \quad (2.9)
$$

where p is the pressure and $\overleftrightarrow{\sigma} = \{\sigma_{ij}\}$ is the dissipative stress tensor expressed in terms of the shear and bulk viscosities η and ζ as

$$
\sigma_{ij} = \eta(\nabla_i v_j + \nabla_j v_i) + (\zeta - 2\eta/3)\delta_{ij}\nabla \cdot \boldsymbol{v}, \quad (2.10)
$$

where $\nabla_i = \partial/\partial x_i$ with $x_i = x, y$, and z. The last term in Eq.(2.8) represents the gravity acceleration with $\boldsymbol{e}_z$ being the unit vector along the z axis. The (total) energy density $e_T = e + \rho\boldsymbol{v}^2/2$ consisting of the internal energy density e and the kinetic energy $\rho\boldsymbol{v}^2/2$ is governed by

$$
\frac{\partial}{\partial t}e_\mathrm{T} = -\nabla \cdot [(e_T + p)\boldsymbol{v} - \overleftrightarrow{\sigma} \cdot \boldsymbol{v} + \boldsymbol{q}] - \rho g v_z \quad (2.11)
$$

where $\boldsymbol{q}$ is the dissipative heat current expressed as [25]

$$
\boldsymbol{q} = -\lambda\nabla T + A\boldsymbol{I}. \quad (2.12)
$$

where λ is the thermal conductivity in the absence of diffusion flux and A is a constant. Because of the symmetry of the Onsager coefficients (see Appendix A), there is a relation between k_T and A given by

$$
k_T = \left[A - \mu + T\left(\frac{\partial\mu}{\partial T}\right)_{cp}\right]\left(\frac{\partial c}{\partial\mu}\right)_{pT}. \quad (2.13)
$$

From Eqs.(2.1) and (2.3) the heat flux and diffusion flux are written as $\boldsymbol{q} \to -\mathcal{Q}\boldsymbol{e}_z$ and $\boldsymbol{I} \to -\mathcal{I}\boldsymbol{e}_z$ far from the bubble $r \gg R$, where

$$
\begin{aligned}
\mathcal{Q} &= \lambda\mathcal{T} + A\mathcal{I}, \quad (2.14) \\
\mathcal{I} &= \rho D(\mathcal{C} + T^{-1}k_T\mathcal{T}). \quad (2.15)
\end{aligned}
$$

The pressure gradient tends to $-\rho g\boldsymbol{e}_z$, while the velocity tends to $-v_D\boldsymbol{e}_z$ because the bubble is at rest in our reference frame. In the present work we linearize the hydrodynamic equations for the velocity field $\boldsymbol{v}$ and the deviations δp, δT, and δc with respect to $\mathcal{T}$, $\mathcal{C}$, and g in steady states in the bulk region $r \neq R$. Here we may set $\partial(\cdots)/\partial t = 0$ neglecting the time-dependence. From Eq.(2.6) it follows the incompressibility condition,

$$
\nabla \cdot \boldsymbol{v} = 0. \quad (2.16)
$$

Then the bulk viscosity ζ does not enter in our calculations. This incompressibility condition holds even in compressible fluids in our linear theory. Notice that we neglect the term $\boldsymbol{v} \cdot \nabla\rho$ in Eq.(2.6) since it is of order $\mathcal{T}g$ in the gravity-induced density stratification. In the bulk region $r \neq R$, Eq.(2.7) and (2.11) yield

$$
\nabla^2\delta T = 0, \quad \nabla^2\delta c = 0, \quad (2.17)
$$

The momentum equation becomes

$$
-\nabla\delta p + \eta\nabla^2\boldsymbol{v} - \rho g\boldsymbol{e}_z = \boldsymbol{0}. \quad (2.18)
$$

The pressure deviation is defined by $\delta p = p - p_0$ for $r > R$ and $\delta p = p - p_0 - 2\gamma_0/R$ for $r < R$. For $r \neq R$, taking the divergence of Eq.(2.18) yields

$$
\nabla^2\delta p = 0. \quad (2.19)
$$

The term $-(\partial\rho/\partial z)g$ is of the second order for $r \neq R$ and is negligible in our approximation.

C. Interface boundary conditions

Next we consider the boundary conditions at the surface $r = R$. In this subsection all the quantities are those at $r = R \pm 0$. In the following equations the quantities at $r = R - 0$ (immediately inside the bubble) are primed

as $\boldsymbol{v}'$, $\delta T'$, $\delta p' \cdots$, while those at $r = R + 0$ (immediately outside the bubble) are unprimed. Hereafter, for any physical quantity $\mathcal{A}$, the symbol,

$$[\mathcal{A}] = \mathcal{A} - \mathcal{A}', \qquad (2.20)$$

denotes the discontinuity of $\mathcal{A}$ at the surface. For example, the entropy difference (per unit mass) and the mass concentration are written as

$$[s] = s - s', \quad [c] = c - c'. \qquad (2.21)$$

The Gibbs-Duhem relation yields $[s]/[c] = -(\partial\mu/\partial T)_{\mathrm{cx},p}$ in terms of the chemical potential difference μ. Hereafter $(\partial \cdots/\partial \cdots)_{\mathrm{cx},p}$ is the derivative taken along the isobaric line on the coexistence surface.

The mass conservation at the surface yields $\boldsymbol{e}_1 \cdot [\rho\boldsymbol{v}] = 0$. It is convenient to introduce the mass flux J through the interface by

$$J = \rho\boldsymbol{e}_1 \cdot \boldsymbol{v} = \rho'\boldsymbol{e}_1 \cdot \boldsymbol{v}', \qquad (2.22)$$

which arises from conversion between gas and liquid. We assume the continuity of the tangential velocity,

$$\boldsymbol{e}_2 \cdot [\boldsymbol{v}] = \boldsymbol{e}_2 \cdot \boldsymbol{v} - \boldsymbol{e}_2 \cdot \boldsymbol{v}' = \boldsymbol{0}. \qquad (2.23)$$

The stress balance at the interface yields

$$[\delta p - \boldsymbol{e}_1 \cdot \overleftrightarrow{\sigma} \cdot \boldsymbol{e}_1] + \frac{2}{R}\delta\gamma = 0, \qquad (2.24)$$

$$[\boldsymbol{e}_2 \cdot \overleftrightarrow{\sigma} \cdot \boldsymbol{e}_1] + \boldsymbol{e}_2 \cdot \nabla\delta\gamma = \boldsymbol{0}, \qquad (2.25)$$

in the normal and tangential directions, respectively. Here $\delta\gamma = \gamma - \gamma_0$ is the surface tension deviation and $\boldsymbol{e}_2 \cdot \nabla = R^{-1}\partial/\partial\theta$. From Eq.(2.25) the tangential gradient of the surface tension is equal to the discontinuity of the tangential stress, which gives rise to a Marangoni flow [1, 24].

As in the pure fluid case [7], we assume that the deviations of the temperature and the chemical potentials are continuous at the interface,

$$\delta T = \delta T', \qquad (2.26)$$

$$\delta\mu_1 = \delta\mu_1' \quad \delta\mu_2 = \delta\mu_2'. \qquad (2.27)$$

See Appendix B of our previous work [7] and the item (i) in the summary section of this work for discussions on the validity of these assumptions. The Gibbs-Duhem relation for infinitesimal deviations is written as $(1 - c)\delta\mu_1 + c\delta\mu_2 = -s\delta T + \rho^{-1}\delta p$, which holds in the liquid and gas regions close to the surface. Further use of Eqs.(2.26) and (2.27) yields

$$[c]\delta\mu + [s]\delta T = \frac{1}{\rho}\delta p - \frac{1}{\rho'}\delta p', \qquad (2.28)$$

where $\delta\mu = \delta\mu_2 - \delta\mu_1$.

From Eq.(2.7) the mass conservation of the second component at the surface gives

$$[c]J + \boldsymbol{e}_1 \cdot [\boldsymbol{I}] = 0. \qquad (2.29)$$

From Eq.(2.11) the energy conservation at the interface gives

$$([s]T + [c]\mu)J + \boldsymbol{e}_1 \cdot [\boldsymbol{q}] = 0, \qquad (2.30)$$

where use has been made of the thermodynamic relation $e + p = \rho_1\mu_1 + \rho_2\mu_2 + \rho s T = (\mu_1 + c\mu + sT)\rho$. From Eqs.(2.29) and (2.30) J may be removed to give

$$\boldsymbol{e}_1 \cdot [\boldsymbol{q} - \alpha T\boldsymbol{I}] = 0, \qquad (2.31)$$

where the coefficient α is defined by

$$\alpha = \mu/T + [s]/[c]. \qquad (2.32)$$

Note that α is a constant continuous across the interface. The flux $\boldsymbol{q} - \alpha T\boldsymbol{I}$ is continuous along the normal direction across the interface.

D. Pressure and surface tension deviations

We shall see that the pressure deviations in the two phases are negligibly small for large R in Eq.(2.28). This yields the following relation,

$$\delta\mu \cong -\frac{[s]}{[c]}\delta T = \left(\frac{\partial\mu}{\partial T}\right)_{\mathrm{cx},p}\delta T, \qquad (2.33)$$

which plays a key role in the following calculations. It may be justified if the hydrodynamic deviations are expanded in powers of the inverse bubble radius R^{-1}. To leading order in R^{-1}, the right hand side of Eq.(2.28) is negligible, resulting in Eq.(2.33).

In equilibrium, the surface tension of binary mixtures is defined on the coexistence surface in the space of three field variables such as T, p, and μ. Here the curvature effect is neglected for large R. Then the surface tension is a function of T and μ if p is taken to be the coexistence pressure $p_{\mathrm{cx}}(T, \mu)$. In Eq.(2.33) the temperature and chemical potential deviations near the interface are still on the coexistence surface in the isobaric condition. Thus the surface tension deviation is written as [27]

$$\begin{aligned} \delta\gamma &= a_1\delta T + a_2\delta\mu \\ &\cong -\gamma_1\delta T, \end{aligned} \qquad (2.34)$$

where a_1 and a_2 are the expansion coefficients. As discussed in Section 1, the coefficient γ_1 is written as

$$-\gamma_1 = a_1 - a_2\frac{[s]}{[c]} = \left(\frac{\partial\gamma}{\partial T}\right)_{\mathrm{cx},p}. \qquad (2.35)$$

III. AXISYMMETRIC SOLUTION

A. Velocity and pressure

In our problem, the fluid flow is axisymmetric with respect to the z axis. The velocity field $\boldsymbol{v}(\boldsymbol{r})$ and the

pressure deviation $\delta p(\boldsymbol{r})$ are expressed in the same forms as in the one-component fluid [7, 26]. That is, in terms of two functions $\hat{Q}(r)$ and $\hat{H}(r)$, $\boldsymbol{v}(\boldsymbol{r})$ is written as

$$\boldsymbol{v} = \left(\frac{d\hat{H}}{dr} - \frac{\hat{H}}{r} + \hat{Q}r\right)\frac{z}{r^2}\boldsymbol{r} + \frac{1}{r}\hat{H}\boldsymbol{e}_z. \qquad (3.1)$$

which satisfies Eq.(2.16). Outside the bubble we have

$$\hat{Q} = Q_1\frac{R}{r^2}, \quad \hat{H} = \frac{R}{2}Q_1 + H_1\frac{R^3}{r^2} - v_{\mathrm{D}}r \quad (r > R). \quad (3.2)$$

where v_{D} is the bubble velocity in the original reference frame. Inside the bubble we have

$$\hat{Q} = Q_2'\frac{r}{R^2}, \quad \hat{H} = -\frac{2}{5R^2}Q_2'r^3 + H_2'r \quad (r < R). \quad (3.3)$$

Then Eq.(2.14) is satisfied. In particular, Eq.(2.16) yields

$$Q_1 = gR^2(\rho - \rho')/3\eta. \qquad (3.4)$$

The coefficients Q_1, H_1, Q_2', and H_2' have the dimension of velocity. From Eqs.(2.18) and (2.19) the pressure deviation is determined as

$$\begin{aligned}
\delta p(r) &= \eta Q_1\frac{Rz}{r^3} - g\rho z \qquad (r > R) \\
&= -2\eta'Q_2'\frac{z}{R^2} - g\rho'z \qquad (r < R). \quad (3.5)
\end{aligned}$$

The mass flux through the interface and the surface tension deviation are angle-dependent as

$$J = J_1\cos\theta, \quad \delta\gamma = \Gamma_1\cos\theta, \qquad (3.6)$$

where $\cos\theta = z/r$ and J_1 and Γ_1 are constants. From the boundary conditions Eq.(2.22)-(2.25), H_1, v_{D}, H_2', and Γ_1 may be expressed in terms of the three quantities J_1, Q_2', and Q_1 as

$$H_1 = \frac{1}{3}\left(\frac{1}{\rho'} - \frac{1}{\rho}\right)J_1 - \frac{1}{15}Q_2' + \frac{1}{6}Q_1, \qquad (3.7)$$

$$v_{\mathrm{D}} = -\frac{1}{3}\left(\frac{2}{\rho'} + \frac{1}{\rho}\right)J_1 + \frac{2}{15}Q_2' + \frac{2}{3}Q_1, \qquad (3.8)$$

$$H_2' = \frac{1}{\rho'}J_1 + \frac{1}{5}Q_2', \qquad (3.9)$$

$$\Gamma_1 = \left(\frac{2}{\rho'} - \frac{2}{\rho}\right)\eta J_1 - \left(\frac{2}{5}\eta + \frac{3}{5}\eta'\right)Q_2' + \eta Q_1. \quad (3.10)$$

Since Q_1 is determined as in Eq.(3.4), the two quantities J_1 and Γ_1 remain unknown.

From Eqs.(2.18) and (2.19) the deviation of the chemical potential difference $\delta\mu$ also satisfies $\nabla^2\delta\mu = 0$ for $r \neq R$. Then δT and $\delta\mu$ are written as

$$\begin{aligned}
\delta T(\boldsymbol{r}) &= (\mathcal{T}' - \mathcal{T})\frac{R^3}{r^3}z + \mathcal{T}z \quad (r > R) \\
&= \mathcal{T}'z \qquad\qquad (r < R), \quad (3.11)
\end{aligned}$$

$$\begin{aligned}
\delta\mu(\boldsymbol{r}) &= (\mathcal{M}' - \mathcal{M})\frac{R^3}{r^3}z + \mathcal{M}z \quad (r > R) \\
&= \mathcal{M}'z \qquad\qquad (r < R), \quad (3.12)
\end{aligned}$$

where $\mathcal{T}$ and $\mathcal{M}$ are the gradients far from the bubble defined in Eqs.(2.1) and (2.3), while $\mathcal{T}'$ and $\mathcal{M}'$ are those within it. At $r = R$, δT and $\delta\mu$ are continuous from Eqs.(2.26) and (2.27). For $r \leq R$ we have

$$\delta T = \mathcal{T}'z, \quad \delta\mu = \mathcal{M}'z. \qquad (3.13)$$

In terms of $\mathcal{T}'$ and $\mathcal{M}'$ the relation Eq.(2.28) is rewritten as

$$[c]\mathcal{M}' + [s]\mathcal{T}' = \left[\frac{\eta}{\rho}Q_1 + \frac{2\eta'}{\rho'}Q_2'\right]\frac{1}{R^2}. \qquad (3.14)$$

Furthermore, we may derive two equations for $\mathcal{T}'$ and $\mathcal{M}'$ from Eqs.(2.29) and (2.30). Together with Eqs.(3.10) and (3.14), we have four equations, which constitute a closed set determining J_1, Q_2', $\mathcal{T}'$, and $\mathcal{M}'$. Here, without assuming Eq.(2.33), we may assume the general relation $\delta\gamma = a_1\delta T + a_2\delta\mu$ in the first line of Eq.(2.34).

B. Case of $g \neq 0$ and $\mathcal{Q} = \mathcal{I} = 0$

Here we consider the gravity-induced solution with $g \neq 0$ and $\mathcal{Q} = \mathcal{I} = 0$, where all the coefficients in Eqs.(3.7)-(3.10) are proportional to Q_1 in Eq.(3.4). If the pressure deviations in Eq.(2.28) are neglected, there arise no deviations of the temperature, the chemical potential, and the surface tension, $\mathcal{T} = \mathcal{T}' = J_1 = \Gamma_1 = 0$. in Eqs.(3.7)-(3.10). Then Eq.(3.10) gives

$$Q_2' = 5\eta Q_1/(2\eta + 3\eta'), \qquad (3.15)$$

while Eq.(3.8) gives $v_D = v_g$, where v_g is the well-known gravity-induced velocity [1, 2, 3].

$$v_g = \frac{2(\eta + \eta')(\rho - \rho')}{3\eta(2\eta + 3\eta')}R^2g. \qquad (3.16)$$

In the lowest order of R^{-1} the right hand side of Eq.(2.28) at $r = R$ becomes

$$\frac{\delta p}{\rho} - \frac{\delta p'}{\rho'} \cong \left[\frac{\eta}{\rho} + \frac{10\eta\eta'}{\rho'(2\eta + 3\eta')}\right]\frac{z}{R^2}Q_1, \qquad (3.17)$$

where the gravity terms cancel to vanish. If divided by Q_1, the above quantity is of order R^{-1}. If we assume the linear relation $\delta\gamma = a_1\delta T + a_2\delta\mu$, the above relation Eq.(3.17) leads to $\delta T \propto \delta\mu \propto Q_1/R$, $\mathcal{T}' \propto \mathcal{M}' \propto Q_1/R^2$, $\Gamma_1 \propto Q_1/R$, and $J_1 \propto Q_1/R^2$. Thus, in the presence of weak gravity only, a large droplet or a large bubble moves with the velocity v_g in Eq.(3.16), where first-order phase transition and temperature inhomogeneities are negligible.

C. Case of $\mathcal{Q} \neq 0$, $\mathcal{I} \neq 0$, and $g = 0$

We seek the solution in the presence of $\mathcal{Q}$ and $\mathcal{I}$ in the gravity-free condition $g = 0$. Remarkably, $\Gamma_1 \propto R$

in binary mixtures with phase change, while $\Gamma_1 \propto R^{-1}$ in one-component fluids. We clarify the relationship of our theory and the previous theories: (i) To obtain the solution without phase change [4], we set $J_1 = 0$ and $\Gamma_1 = -\gamma_1 RT' \propto R$ in Eqs.(3.7)-(3.10) and require the energy conservation relation $\boldsymbol{e}_1 \cdot [\boldsymbol{q}] = 0$ from Eq.(2.30). (ii) To obtain the solution for one-component fluids with phase change [7], we neglect Γ_1 and retain J_1 in Eq.(3.10).

We use the relation Eq.(2.33) or neglect the right hand side of Eq.(3.14) to obtain

$$\mathcal{M}' = -\mathcal{T}'[s]/[c]. \qquad (3.18)$$

The above relation will be justified self-consistently at the end of this subsection. From Eqs.(2.34) and (3.13) Γ_1 in Eqs.(3.6) and (3.10) is expressed as

$$\Gamma_1 = -\gamma_1 R\mathcal{T}'. \qquad (3.19)$$

As will be shown in Appendix B, $\mathcal{T}'$ can be written as

$$\mathcal{T}' = \frac{3}{2\lambda_e + \lambda'_e}(\mathcal{Q} - \alpha T \mathcal{I}), \qquad (3.20)$$

where $\mathcal{Q}$ and $\mathcal{I}$ are defined by Eqs.(2.14) and (2.15). We introduce the effective thermal conductivity by

$$\lambda_e = \lambda + \frac{\rho D}{T}\left(\frac{\partial \mu}{\partial c}\right)_{Tp}(k_T + Z)^2. \qquad (3.21)$$

The λ_e and λ'_e in Eq.(3.20) are the values of λ_e at $r = R + \pm 0$. In Eq.(3.21) we define Z by

$$\frac{Z}{T} = \left(\frac{\partial c}{\partial T}\right)_{\mu p} - \left(\frac{\partial c}{\partial \mu}\right)_{Tp}\frac{[s]}{[c]} = \left(\frac{\partial c}{\partial T}\right)_{cx,p}. \qquad (3.22)$$

On the other hand, the mass flux through the interface J is calculated from Eq.(2.29) or Eq.(2.30). Then J_1 in Eq.(3.6) is expressed as

$$J_1 = 3\frac{(2\lambda_a + \lambda'_a)\mathcal{I} - (2B + B')\mathcal{Q}}{[c](2\lambda_e + \lambda'_e)}, \qquad (3.23)$$

where λ_a, λ'_a, B, and B' are the values of λ_a and B at $r = R + \pm 0$ with

$$\lambda_a = \lambda_e + \alpha T B = \lambda + AB, \qquad (3.24)$$
$$B = \rho D(k_T + Z)/T. \qquad (3.25)$$

From Eq.(3.10) we obtain

$$Q'_2 = \frac{5}{2\eta + 3\eta'}\left[\gamma_1 RT' + (\frac{2}{\rho'} - \frac{2}{\rho})\eta J_1\right]. \qquad (3.26)$$

Substitution of the above relation into Eq.(3.8) yields the drift velocity composed of two parts,

$$v_D = v_D^M + v_D^c, \qquad (3.27)$$

where v_D^M arises from the Marangoni effect and v_D^c from the evaporation-condensation. They are written as

$$v_D^M = \frac{2\gamma_1}{3(2\eta + 3\eta')}R\mathcal{T}', \qquad (3.28)$$

$$v_D^c = \frac{-2}{2\eta + 3\eta'}\left(\frac{\eta}{\rho} + \frac{\eta'}{2\rho} + \frac{\eta'}{\rho'}\right)J_1. \qquad (3.29)$$

In terms of these characteristic velocities, the velocity field $\boldsymbol{v}(\boldsymbol{r})$ in the reference frame moving with the bubble or the droplet is expressed as

$$\boldsymbol{v} = v_D^M \boldsymbol{a}_M + \frac{\eta(\rho' - \rho)v_D^c}{\eta\rho' + \eta'(\rho + \rho'/2)}\boldsymbol{a}_c - (v_D^M + v_D^c)\boldsymbol{e}_z, \quad (3.30)$$

where $\boldsymbol{a}_M = \boldsymbol{a}_M(\boldsymbol{r})$ and $\boldsymbol{a}_c = \boldsymbol{a}_c(\boldsymbol{r})$ are the following space-dependent dimensionless vectors,

$$\boldsymbol{a}_M = -\frac{R^3}{2r^3}\boldsymbol{e}_z + \frac{3R^3}{2r^5}z\boldsymbol{r} \quad (r > R)$$
$$= \frac{5}{2}\boldsymbol{e}_z - \frac{3r^2}{R^2}\boldsymbol{e}_z + \frac{3}{2R^2}z\boldsymbol{r} \quad (r < R), \quad (3.31)$$
$$\boldsymbol{a}_c = \frac{\eta'}{2\eta}\left[\frac{R^3}{r^3}\boldsymbol{e}_z - \frac{3R^3}{r^5}z\boldsymbol{r}\right] \quad (r > R)$$
$$= \frac{z\boldsymbol{r}}{R^2} + \left[2 + \frac{\eta'}{2\eta} - \frac{2r^2}{R^2}\right]\boldsymbol{e}_z \quad (r < R), \quad (3.32)$$

We may now show that the right hand side of Eq.(3.14) is surely negligible for large R. Use of Eq.(3.26) gives

$$\frac{\delta p}{\rho} - \frac{\delta p'}{\rho'} = \frac{10\eta'}{2\eta + 3\eta'}\left[\frac{\gamma_1 \mathcal{T}'}{\rho' R} + (\frac{2}{\rho'} - \frac{2}{\rho})\frac{\eta J_1}{\rho' R^2}\right]. \quad (3.33)$$

We compare the term ($\propto R^{-1}\mathcal{T}'$) on the right hand side of Eq.(3.33) and the term $[s]\mathcal{T}'$ on the left hand side of Eq.(3.14). The former is much smaller than the latter for $R \gg |\gamma_1/\rho'[s]|$, where the right hand side is microscopic. The term ($\propto R^{-2}J_1$) due to the evaporation-condensation in Eq.(3.33) is also negligible, as already verified in our previous paper [7].

The concentration deviation $\delta c(\boldsymbol{r})$ can also be expressed in the same form as in Eqs.(3.11) and (3.12), where the gradient $\mathcal{C}$ far from the droplet satisfies Eq.(2.3), Its values at $r = R \pm 0$ are written as $\delta c_\pm$ and are expressed as

$$\delta c_+ = \frac{Z}{T}\mathcal{T}'z, \quad \delta c_- = \frac{Z'}{T}\mathcal{T}'z, \qquad (3.34)$$

where Z and Z' are the values of Z in Eq.(3.22) at $r = R \pm 0$. If $Z \neq Z'$, δc is discontinuous at $r = R$.

We note that the Marangoni effect vanishes in azeotropic mixtures [26], where the two phases have the same composition or $[c] = 0$. There is also no difference in the molar fractions of the two phases (see the sentence below Eq.(C3)). Special analysis is thus needed when we treat nearly azeotropic mixtures. For example, in H_2O-D_2O mixtures, the relative composition change $[c]/c$ is only 0.5% of the relative density change $[n]/n$ near the

critical line [17]. Thus let us consider the limit $[c] \to 0$ in the equations in this subsection. Then $Z \sim [c]^{-1}$ and $\lambda_e \sim [c]^{-2}$ from Eqs.(3.20) and (3.21), leading to $\Gamma_1 \sim \gamma_1 [c]^2$, $\mathcal{T}' \sim [c]^2 (\mathcal{Q} - \alpha T \mathcal{I})$, and

$$v_D^M \sim \gamma_1 [c]^2 R (\mathcal{Q} - \alpha T \mathcal{I}). \tag{3.35}$$

from Eqs.(3.19), (3.20), and (3.28). Here $\gamma_1 \sim [c]^{-1}$ [12] and $\gamma_1 [c]^2 \sim [c]$, so the Marangoni flow is of order $[c]$.

IV. DILUTE MIXTURES IN GAS-LIQUID COEXISTENCE

Let the second component be a dilute solute. Under the condition Eq.(A8) we set

$$c \cong m_2 X / m_1, \tag{4.1}$$
$$(\partial c / \partial \mu)_{Tp} \cong m_2^2 X / m_1 T, \tag{4.2}$$

where X is the molar fraction and m_1 and m_2 are the molecular masses. The second relation (4.2) does not hold very close to the solvent criticality even for small X (see Eq.(C7)). Hereafter the Boltzmann constant will be set equal to unity. In the literature [12, 13, 14, 15, 16, 17], Henry's law is expressed in terms of the solute molar fractions. That is, in equilibrium, the solute molar fraction in gas X_g and that in liquid X_ℓ are related by the partition coefficient [12],

$$\mathcal{K} = X_g / X_\ell, \tag{4.3}$$

which depends on T along the solvent coexistence line $p = p_{\text{cx}}(T)$. In dilute mixtures $[c]/c = [X]/X$ holds and $[c]/c$ is independent of c as

$$[c]/c = 1 - \mathcal{K} \quad \text{(gas bubble)}$$
$$= 1 - \mathcal{K}^{-1} \quad \text{(liquid droplet)}. \tag{4.4}$$

A. Expressions as $c \to 0$

To simplify the notation we introduce the following dimensionless parameter,

$$\mathcal{W} = \frac{[X]}{X[\sigma]} = \frac{[c]}{cm_1[s]}, \tag{4.5}$$

where $\sigma = m_1 s$ is the entropy per solvent particle. This parameter tends to a well-defined limit in the dilute limit, vanishes for azeotropic mixtures, and becomes proportional to the Krichevskii parameter K_{Kr} near the solvent criticality as in Eq.(C6) in Appendix C. In Eq.(3.22) Z behaves in terms of $\mathcal{W}$ as

$$Z \cong -\frac{m_2 c[s]}{[c]} = -\frac{m_2}{m_1 \mathcal{W}}. \tag{4.6}$$

From Eq.(3.21) λ_e is inversely proportional to c as

$$\lambda_e \cong \frac{\rho D_0}{m_2 c} Z^2 \cong \frac{n D_0}{\mathcal{W}^2 X}, \tag{4.7}$$

where $D_0 = \lim_{c \to 0} D$ is the diffusion constant of a single solute molecule and $n = \rho / m_1$ is the solvent number density. The thermal conductivity λ in Eq.(3.21) is smaller than the right hand side of Eq.(4.7), as will be discussed in Appendix C. Here, in calculating the flux $e_1 \cdot (q - \alpha T I)$ in Eq.(2.31), we have picked up the contribution from the solute diffusion to obtain λ_e in Eq.(4.7).

Furthermore, λ_a in Eq.(3.24) and B in Eq.(3.25) are finite as $c \to 0$. From Eq.(3.20) we thus find $\mathcal{T}' \propto c$ as

$$\mathcal{T}' \cong A_M c \left(\mathcal{Q} - T \frac{[s]}{[c]} \mathcal{I} \right). \tag{4.8}$$

Here we have set $\alpha \cong [s]/[c]$ from Eq.(2.32) assuming that $\mathcal{I}$ is of order c. The coefficient A_M is a positive constant independent of c as $c \to 0$ and is defined by

$$A_M = \frac{3 \mathcal{W}^2 m_1 / m_2}{2 n D_0 + X' n' D_0' / X}, \tag{4.9}$$

which is expressed in terms of the molar fractions X and X' outside and inside the domain. The mass flux through the interface J in Eq.(2.22) tends to that of the pure fluid as $c \to 0$. That is, J_1 in Eq.(3.6) becomes

$$J_1 = (3/[s]T) \mathcal{Q}. \tag{4.10}$$

Now the two drift velocities v_D^M in Eq.(3.28) and v_D^c in Eq.(3.29) are written as

$$v_D^M = \frac{2 A_M \gamma_1}{3(2\eta + 3\eta')} cR \left(\mathcal{Q} - \frac{[s]}{[c]} T \mathcal{I} \right), \tag{4.11}$$

$$v_D^c = \frac{-6}{2\eta + 3\eta'} \left(\frac{\eta}{\rho} + \frac{\eta'}{2\rho} + \frac{\eta'}{\rho'} \right) \frac{\mathcal{Q}}{[s]T}. \tag{4.12}$$

From Eq.(3.34) the deviation of the mass fraction δc at $r = R \pm 0$ are expressed as

$$\frac{\delta c_+}{c} = \frac{\delta c_-}{c'} = -\frac{m_2[s]}{[c]} \mathcal{T}' z. \tag{4.13}$$

Thus $\delta c / c$ is continuous and $[\delta c] = -m_2[s] \delta T$ at $r = R$ to leading order in R^{-1}. In our linear theory we require $|\delta c| \ll c$, which becomes $|\mathcal{T}'| R \ll |[c]/m_2[s]|$. From Eq.(4.8) this inequality is satisfied for small $\mathcal{Q}$ and $\mathcal{I}$ even as $c \to 0$.

Let us consider situations in which the diffusion flux $\mathcal{I}$ is negligible in v_D^M in Eq.(4.11). Then v_D^M and v_D^c have the same sign for a bubble with $\gamma_1 > 0$ and for a liquid droplet with $\gamma_1 < 0$, while they have different signs for a bubble with $\gamma_1 < 0$ and for a liquid droplet with $\gamma_1 > 0$. In accord with the experiments [21, 22, 23], bubbles can move towards cooler regions with increasing the concentration of a solute in the case $\gamma_1 < 0$.

B. Dilute mixtures near the solvent criticality

The above expressions can be used even in the vicinity of the solvent criticality under the condition $X \ll$

$n/\mathcal{W}^2 C_p$ in Eq.(C8), where C_p is the isobaric specific heat per unit volume. In the near-critical case, the reduced temperature,

$$\epsilon = 1 - T/T_c, \qquad (4.14)$$

is small (say, less than 10^{-3}) and the differences between the two phases tend to vanish, so $\rho' \cong \rho$ and $\eta' \cong \eta$. In Eq.(4.9) we have

$$A_M \cong \mathcal{W}^2 m_1/m_2 n D_0. \qquad (4.15)$$

Defining the solute hydrodynamic radius a_0 using the Stokes formula $D_0 = T/6\pi\eta a_0$, we obtain

$$v_D^M = \frac{4\pi}{5nT} \mathcal{W}^2 \gamma_1 a_0 RX \left(\mathcal{Q} - \frac{[s]}{[c]} T\mathcal{I} \right), \quad (4.16)$$

$$v_D^c = -3\mathcal{Q}/nT[\sigma], \qquad (4.17)$$

where $[\sigma] = m_1[s] \sim \epsilon^\beta$.

With increasing X from zero, crossover occurs from the pure-fluid behavior to the mixture-behavior for $X > X^*$, where the crossover molar fraction is

$$X^* = (\epsilon^\beta |\gamma_1| \mathcal{W}^2 a_0)^{-1} R^{-1}. \qquad (4.18)$$

This is equivalent to Eq.(1.6) near the solvent criticality with $c^* = m_2 X^*/m_1 \sim X^*$ if $|\mathcal{W}| \sim 1$ and $m_2 \sim m_1$. The right hand side is of order $\epsilon^{1-\nu-\beta}\xi/R$ for $|\mathcal{W}| \sim 1$ and $\gamma_1 \sim -d\gamma_0/dT$ with $\nu \cong 0.625$ and $\beta \cong 0.33$, $\xi(\sim \epsilon^{-\nu})$ being the correlation length ($\sim$the interface thickness).

In near-critical pure fluids in the gravity-free condition, a bubble in liquid was observed to be attracted to a warmer boundary [9]. With addition of a small amout of various solutes, it is then of great interest whether a bubble is more attracted to or eventually repelled from a warmer boundary. Here the crossover concentration X^* should be measured to confirm the theoretical expression (4.18).

-

V. VELOCITY PROFILES FOR $\mathcal{Q} \neq 0$, $\mathcal{I} \neq 0$, AND $g = 0$

Young et al. [4] calculated the velocity field without phase change due to the Marangoni effect for $\gamma_1 > 0$ (which is given by Eq.(3.30) with $v_D^c = 0$). See its dipolar profile in their paper and in our previous paper [7]. On the other hand, our previous paper [7] has presented some examples of the velocity field due to first-order phase change for pure fluids (which is given by Eq.(3.30) with $v_D^M = 0$). Here we display the velocity fields realized in dilute mixtures with increasing c or in nearly azeotropic mixtures.

Without gravity, we show the velocity field (v_x, v_z) in the x-z plane for a bubble with $\rho'/\rho = \eta'/\eta = 0.5$ in Fig.1 and for a liquid droplet with $\rho'/\rho = \eta'/\eta = 2$ in Fig.2. It is written in the reference frame moving with a bubble

or a droplet in the case $v_D^c < 0$. Here the liquid density is twice larger than the gas density, which is realized for $T/T_c = 0.97$ in the van der Waals theory of pure fluids. In the left panels, we set $v_D^M = 0$ for pure fluids or for $\gamma_1 = 0$ in binary mixtures. In the middle panels, we set $v_D^M = v_D^c$, where the two mechanisms equally contribute to the drift velocity. In the right panels, we set $v_D^M = -v_D^c$, where the drift velocity v_D in Eq.(3.27) vanishes and the bubble or the droplet is at rest.

VI. SUMMARY AND REMARKS

We have examined the competition of the evaporation-condensation effect and the Marangoni effect in the motion of a bubble or a droplet in weak heat and diffusion fluxes in binary mixtures. We have treated the simplest case of steady states with a constant drift velocity in the axisymmetric geometry, though the nonlinear terms in the hydrodynamic equations cannot be neglected in practical applications using large bubbles. In non-azeotropic binary mixtures, the crossover occurs from the evaporation-condensation mechanism to the Marangoni mechanism at a very small solute concentration. In our theory, the coefficient γ_1 in Eq.(1.3) controls the strength of the Marangoni flow in heat flux, which can be both positive and negative depending on the solvent and solute species [12]. The Marangoni flow is induced in opposite directions in the normal case $\gamma_1 > 0$ and in the anomalous case $\gamma_1 < 0$, though the case $\gamma_1 > 0$ has mostly been studied.

Some further remarks are given below.
(i) We have assumed the continuity of the temperature and the chemical potentials and neglected the pressure deviations at the interface to obtain the key relation Eq.(2.33) or Eq.(3.18). It means that the interface stays on the coexistence surface $p = p_{cx}(T, \mu)$ even in nonequilibrium. This is justified for large R. However, if the gas phase is very dilute far below the critical temperature, the surface dissipation mainly occurs in the gas phase side within a distance of the mean-free path inversely proportional to the gas density [28, 29, 30]. There can then be an apparent temperature jump at the interface.
(ii) The behavior of the coefficient γ_1 in Eq.(1.3) or in Eq.(2.35) is highly nontrivial. Theoretically, it has been examined only for dilute mixtures [12]. Its behavior is also of interest for binary mixtures near a lower critical solution temperature (LCST). In a phase-separated mixture of butoxyethanol-water near its LCST, Braun et al. [31] applied heat-pulses to water-rich droplets to observe their motion from a high-temperature region to a low-temperature region. This motion was due to the Marangoni effect because the motion was in the direction of decreasing the surface tension.
(iii) Boiling on a heated substrate has been of great interest both on earth and in space [32]. The effect of a noncondensable gas should be studied in future. In
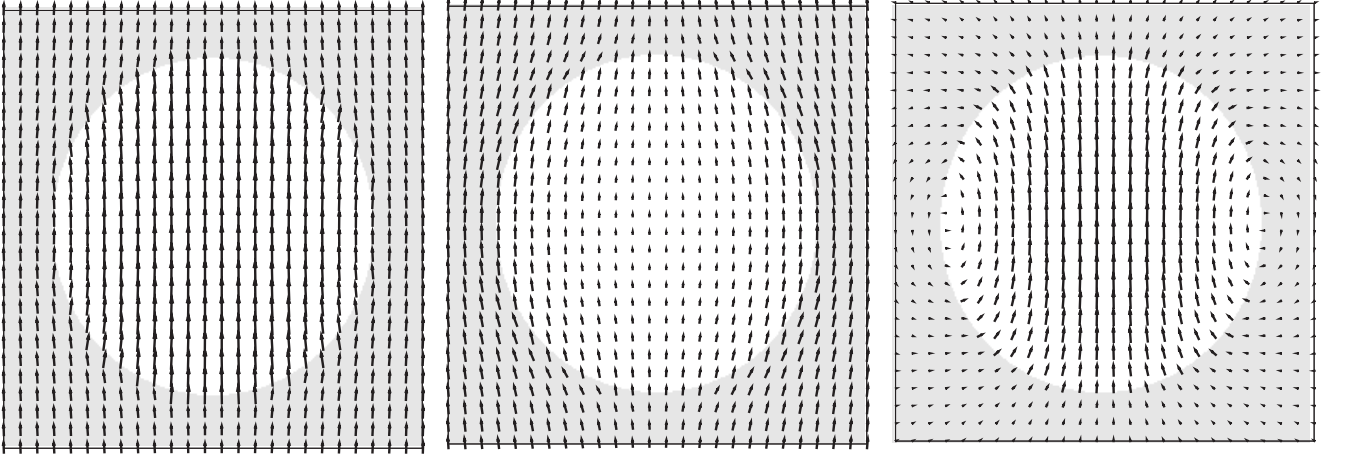
FIG. 1: Gravity-free velocity field around a bubble for $\eta'/\eta = \rho'/\rho = 0.5$ in the x-z plane in Eqs.(3.30)-(3.32), where $v_D^M = 0$ (left), $v_D^M = v_D^c$ (middle), and $v_D^M = -v_D^c$ (right).
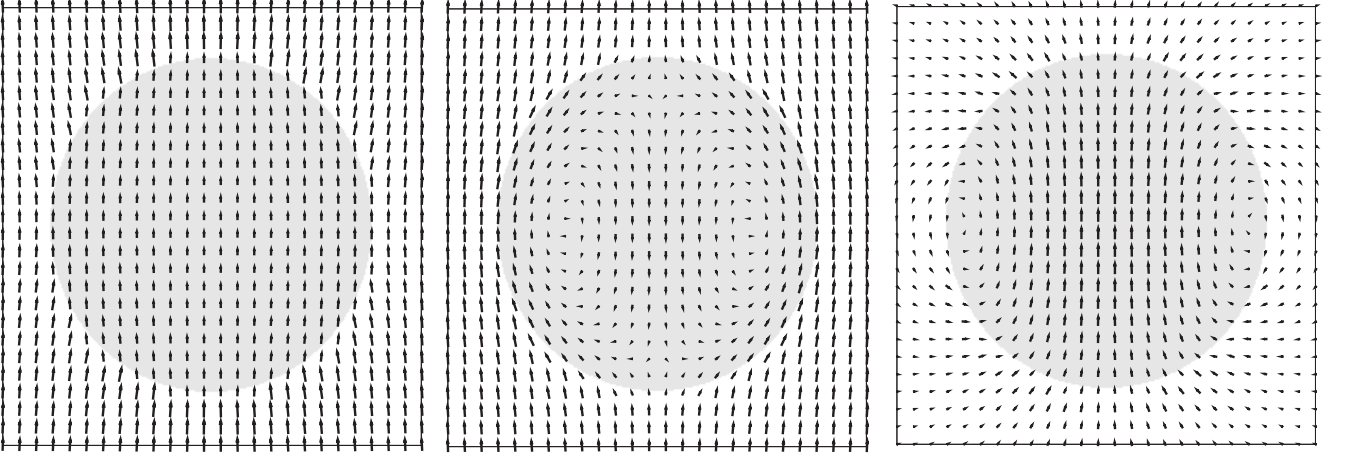

FIG. 2: Gravity-free velocity field around a liquid droplet for $\eta'/\eta = \rho'/\rho = 2$ in the x-z plane in Eqs.(3.30)-(3.32), where $v_D^M = 0$ (left), $v_D^M = v_D^c$ (middle), and $v_D^M = -v_D^c$ (right).

accord with this paper, Marek and Starub [10] claimed that the temperature gradients along the bubble interface inducing a Marangoni flow are caused by saturation pressure gradients due to a nonuniform accumulation of a noncondensable gas along the interface. Such flow serves to suppress detachment of bubbles for $\gamma_1 > 0$, but should accelerate it for $\gamma_1 < 0$ [21].

(iv) In gravity-free conditions, a spherical bubble or droplet can be suspended in liquid or gas in equilibrium. It is of great interest how the velocity field and temperature evolve after application of heat flux from a boundary. The piston effect comes into play on acoustic time scales [26, 33]. On longer time scales, a small amount of a solute should drastically change the hydrodynamic behavior inducing a Marangoni flow. However, since we have treated only steady states, it remains unclear how the concentration changes in time along the interface.

(v) Thermocapillary hydrodynamics has been puzzling near the critical point [9, 26, 33], where the singularities of the thermodynamic and dynamical properties largely influence the dynamics. The condition (4.2) or the condition (C8) does not hold sufficiently close to the critical point, where the results in Section 4 cannot be used. Thus, with addition of a solute, two-phase hydrodynamics poses a new problem of critical dynamics.

(vi) Finally, we should stress that surfactant molecules absorbed at interfaces give rise to Marangoni flow [1, 11], though this effect is beyond the scope of this paper.

Appendix A: Onsager relations

In the linear response theory, the dissipative heat and diffusion fluxes, $\boldsymbol{q}$ and $\boldsymbol{I}$, in binary mixtures are expressed in terms of the Onsager kinetic coefficients L_{ij} [25]. The thermodynamic forces are ∇T and $\nabla(\mu/T)$ as

$$\boldsymbol{q} = -L_{11}\nabla T - TL_{12}\nabla\frac{\mu}{T}, \qquad (A1)$$

$$\boldsymbol{I} = -L_{12}\frac{1}{T}\nabla T - L_{22}\nabla\frac{\mu}{T}, \qquad (A2)$$

where $\mu = \mu_2 - \mu_1$ with μ_i being the chemical potentials per unit mass. We then consider the dynamic equation for the entropy density $S = \rho s$ per unit volume. The thermodynamic relation $TdS = de - \mu_1 d\rho_1 - \mu_2 d\rho_2$ and the hydrodynamic equations yield

$$\frac{\partial}{\partial t}S + \nabla \cdot \left(S\boldsymbol{v} + \frac{1}{T}\boldsymbol{q} - \frac{\mu}{T}\boldsymbol{I}\right) = \frac{1}{T}\dot{\epsilon}, \qquad (A3)$$

where $\dot{\epsilon}$ is the heat production rate per unit volume expressed as

$$\dot{\epsilon} = \sum_{ij} \sigma_{ij}\frac{\partial v_i}{\partial x_j} - \boldsymbol{q}\cdot\frac{\nabla T}{T} - T\boldsymbol{I}\cdot\nabla\frac{\mu}{T}. \qquad (A4)$$

The first term arises from the viscous damping and the last two terms from the heat conduction and diffusion. As is well-known, $\dot{\sigma}$ is nonnegative-definite if the coefficients L_{ij} constitute a symmetric positive-definite 2×2 matrix. It is well-known that L_{ij} are expressed in terms of the the time-integral of the appropriate flux time-correlations (Green-Kubo formulas) [26].

It is convenient to express $\boldsymbol{q}$ as in Eq.(2.12) and $\boldsymbol{I}$ as in Eq.(2.8). Then λ, A, D, and k_T are expressed as

$$\lambda = L_{11} - L_{12}^2/L_{22}, \qquad (A5)$$

$$A = TL_{12}/L_{22}, \qquad (A6)$$

$$\rho T D = L_{22}\left(\frac{\partial\mu}{\partial c}\right)_{pT}, \qquad (A7)$$

$$\rho D k_T = L_{12} - \frac{\mu}{T}L_{22} + \left(\frac{\partial\mu}{\partial T}\right)_{cp}L_{22}. \qquad (A8)$$

If L_{12} and L_{22} are removed from Eqs.(A6)-(A8), k_T and A are related as in Eq.(2.13).

Appendix B: Calculations of $\mathcal{T}'$ and J_1

To derive Eq.(3.20) we calculate the heat and diffusion fluxes at the interface in the normal direction substituting Eqs.(3.11) and (3.12) into Eqs.(A1) and (A2) and setting $\mathcal{M}' = -\mathcal{T}'[s]/[c]$ from Eq.(3.14) for large R. The unprimed quantities are the values at $r = R + 0$, while the primed ones are those at $r = R - 0$.

From Eq.(3.11) the gradient $\boldsymbol{e}_1 \cdot \nabla\delta T$ normal to the interface is $(3\mathcal{T} - 2\mathcal{T}')\cos\theta$ for $r = R + 0$ and to $\mathcal{T}'\cos\theta$ for $r = R - 0$. From Eq.(3.12) the gradient $\boldsymbol{e}_1 \cdot \nabla\delta\mu$

is obtained by replacement of $\mathcal{T}'$ and $\mathcal{T}$ by $\mathcal{M}'$ and $\mathcal{M}$. Then use of Eqs.(3.11)-(3.14) gives

$$\begin{aligned}\boldsymbol{e}_1 \cdot \boldsymbol{q} &= (2\lambda_a\mathcal{T}' - 3\mathcal{Q})\hat{z} \quad (r = R+0), \\ &= -\lambda_a'\mathcal{T}'\hat{z} \quad (r = R-0), \qquad (B1) \\ \boldsymbol{e}_1 \cdot \boldsymbol{I} &= (2B\mathcal{T}' - 3\mathcal{I})\hat{z} \quad (r = R+0), \\ &= -B'\mathcal{T}'\hat{z} \quad (r = R-0) \qquad (B2)\end{aligned}$$

where $\hat{z} = z/r = \cos\theta$. We define $\mathcal{Q}$ and $\mathcal{I}$ in Eqs.(2.14) and (2.15) and introduce

$$\lambda_a = L_{11} - \alpha L_{12} = \lambda + L_{12}(A/T - \alpha), \qquad (B3)$$

$$B = (L_{12} - \alpha L_{22})/T = L_{22}(A/T - \alpha)/T. \qquad (B4)$$

The flux $\boldsymbol{q} - T\alpha\boldsymbol{I}$ along $\boldsymbol{e}_1$ in Eq.(2.31) may then be calculated at $r = R \pm 0$. Its continuity at $r = R$ gives

$$(2\lambda_e + \lambda_e')\mathcal{T}' - 3(\mathcal{Q} - T\alpha\mathcal{I}) = 0. \qquad (B5)$$

Here λ_e is the effective thermal conductivity defined by

$$\begin{aligned}\lambda_e &= \lambda_a - \alpha BT \\ &= \lambda + L_{22}(A/T - \alpha)^2, \qquad (B6)\end{aligned}$$

where use of Eqs.(2.13) and (2.32) yields

$$\begin{aligned}\frac{A}{T} - \alpha &= \left(\frac{\partial\mu}{\partial c}\right)_{Tp}\frac{k_T}{T} - \left(\frac{\partial\mu}{\partial T}\right)_{cp} - \frac{[s]}{[c]} \\ &= \frac{1}{T}\left(\frac{\partial\mu}{\partial c}\right)_{Tp}(k_T + Z). \qquad (B7)\end{aligned}$$

From $(\partial c/\mu)_{Tp}(\partial\mu/\partial T)_{cp} = -(\partial c/\partial T)_{\mu p}$ and Eq.(A7) we obtain Z in Eq.(3.22) and λ_e in Eq.(3.21). From Eqs.(2.29) and (3.6) J_1 in the mass flux through the interface is determined by

$$\begin{aligned}J_1 &= [3\mathcal{Q} - (2\lambda_a + \lambda_a')\mathcal{T}']/T[c]\alpha \\ &= [3\mathcal{I} - (2B + B')\mathcal{T}']/[c], \qquad (B8)\end{aligned}$$

which yields Eq.(3.23) with the aid of Eq.(3.20).

Appendix C: Mass and molar fractions and relations in near-critical dilute mixtures

In hydrodynamic theory the mass fraction c and the chemical potential difference μ per unit mass are usually used, but in thermodynamics it is convenient to use the molar fraction X and the chemical potential difference Δ per particle. In terms of the molecular masses m_1 and m_2 they are related by [26]

$$c = m_2 X/[m_1(1 - X) + m_2 X], \qquad (C1)$$

$$\Delta = m_2\mu_2 - m_1\mu_1. \qquad (C2)$$

At any concentration it generally holds the relation,

$$\left(\frac{\partial c}{\partial\mu}\right)_{TP} = m_1^2 m_2^2(n/\rho)^3\left(\frac{\partial X}{\partial\Delta}\right)_{TP}. \qquad (C3)$$

We also note the relation $[c] = [X](m_1 cc'/m_2 XX')$. The azeotropy condition $[X] = 0$ is also given by $[c] = 0$.

First we give thermodynamic relations in dilute mixtures with $c \ll 1$. In the text of this paper we assume Eqs.(4.1) and (4.2). To describe the critical behavior, it is convenient to introduce the Krichevskii parameter K_{Kr}, which is the dilute limit of the thermodynamic derivative $(\partial p/\partial X)_{nT}$ at fixed $n = n_1 + n_2$ and T at the solvent criticality [13, 14, 15, 16, 17]. It is related to the derivatives of the critical pressure p_c and the critical temperature T_c with respect to X along the critical line as

$$K_{\mathrm{Kr}} = \frac{dp_c}{dX} - p'_{\mathrm{cx}}\frac{dT_c}{dX}, \qquad (C4)$$

where $p'_{\mathrm{cx}} = dp_{\mathrm{cx}}/dT$ is the temperature-derivative of the coexistence pressure $p_{\mathrm{cx}}(T)$ of the pure fluid. The Clausius-Clapeyron relation $p'_{\mathrm{cx}} = [\sigma]/[v]$ holds for the pure fluid, where $v = 1/n$ is the inverse density and σ is the entropy per particle. In near-critical two-phase coexistence, the mass fraction difference $[X]$ and the volume difference $[v]$ are related by [12]

$$[X]/[v] = (K_{\mathrm{Kr}}/T_c)X_c, \qquad (C5)$$

where $X_c = (X_g + X_\ell)/2$ is the critical value of X [12]. Thus the parameter $\mathcal{W}$ in Eq.(4.5) is expressed near the criticality as

$$\mathcal{W} = K_{\mathrm{Kr}}[v]/T_c[\sigma] = K_{\mathrm{Kr}}/T_c p'_{\mathrm{cx}}. \qquad (C6)$$

On the other hand, the the thermodynamic derivative $(\partial X/\partial \Delta)_{Tp}$ behaves as [26]

$$\left(\frac{\partial X}{\partial \Delta}\right)_{pT} \cong \frac{X}{T} + \frac{X^2}{nT^2}K_{\mathrm{cr}}^2 K_{T\Delta}. \qquad (C7)$$

where $K_{T\Delta} = (\partial n/\partial p)_{T\Delta}/n$ is the isothermal compressibility growing strongly near the criticality. On the right hand side of Eq.(C7), the first term is the dilute limit, while the second term is the singular contribution stemming from the solute-solvent interaction and can be important very close to the criticality. In this paper we neglect the second term in Eq.(C7), which is allowable under the condition,

$$X \ll \frac{nT}{K_{\mathrm{cr}}^2 K_T} \cong \frac{n}{\mathcal{W}^2 C_p}, \qquad (C8)$$

where $K_T = (\partial n/\partial p)_T/n$ is the isothermal compressibility and $C_p = \rho T(\partial s/\partial T)_p \cong T(p'_{\mathrm{cx}})^2 K_T$ is the isobaric heat capacity per unit volume of the pure fluid [26]. However, the reverse relation $X > n/\mathcal{W}^2 C_p$ eventually holds sufficiently close to the criticality.

Next we consider the dynamic properties of dilute mixtures. The Onsager coefficients L_{12} and L_{22} are proportional to c, while L_{11} tends to the thermal conductivity of the pure fluid. Thus, as $c \to 0$, A in Eq.(A6) and D in Eq.(A7) tend to well-defined limits, while k_T in Eq.(A8) is proportional to c as

$$k_T = k_T^* c, \qquad (C9)$$

with k_T^* being a constant independent of c. The singular part of L_{22} (proportional to X^2) is negligible compared to the background part under Eq.(C8) [26], so that

$$L_{22} \cong m_2 \rho c D_0, \qquad (C10)$$

where D_0 is the diffusion constant of a single solute particle in the dilute limit. The thermal conductivity λ in Eq.(A5) behaves in a dilute binary mixture near the solvent criticality as [26]

$$\lambda \cong \lambda_s \lambda_B/(\lambda_s + \lambda_B). \qquad (C11)$$

Here λ_s is the thermal conductivity of the pure fluid growing strongly near the solvent criticality and $\lambda_B = \lambda_{B0}/X$ is the critical value inversely proportional to c with λ_{B0} being a constant. The mode-coupling theory of critical dynamics predicted the growing behavior $\lambda_s \cong TC_p/6\pi\eta\xi \sim \xi$, where ξ is the correlation length and $C_p(\sim K_T)$ is the isobaric heat capacity per unit volume. We then recognize that the effective thermal conductivity λ_e in Eq.(3.21) may be approximated as Eq.(4.6) under Eq.(C8). Using Eq.(C8) and the hydrodynamic radius a_0 in the Stokes formula $D_0 = T/6\pi\eta a_0$, we can make the following estimation,

$$\frac{\lambda_e}{\lambda} > \frac{\lambda_e}{\lambda_s} \sim \frac{nD_0}{\mathcal{W}^2 X\lambda_s} \sim \frac{n\xi/a_0}{C_p\mathcal{W}^2 X} \gg 1. \qquad (C12)$$

[1] B. Levich, *Physicochemical Hydrodynamics* (Prentice-Hall, Englewood Cliffs, N.J., 1962).
[2] J. Hadamard, C.R. Acad. Sci., Paris, **152**, 1735 (1911).
[3] D. Rybczynski, Bull. Acad. Sci. Cracovie, **1**, 40 (1911).
[4] N. O. Young, J. S. Goldstein, and M. J. Block, J. Fluid Mech. **6**, 350 (1959).
[5] G. Wozniak, R. Balasubramaniam, P. H. Hadland, and R. S. Subramanian, Exp. Fluids **31**, 84 (2001).
[6] N. Ichikawa, M. Kawaji, and M. Misawa, Microgravity Science Technol. **14**, 34 (2003).
[7] A. Onuki and K. Kanatani, Phys. Rev. E, **72**, 066304 (2005).
[8] A. Onuki, Phys. Rev. Lett. **94**, 054501 (2005); Phys. Rev. E **75**, 036304 (2007); R. Teshigawara and A. Onuki, Europhys. Lett. **84**, 36003 (2008).
[9] Y. Garrabos, C. Lecoutre-Chabot, J. Hegseth, V. S. Nikolayev, D. Beysens, and J.-P. Delville Phys. Rev. E **64**, 051602 (2001).

[10] R. Marek and J. Straub, Int. J. of Heat and Mass Transfer, **44**, 619 (2002).

[11] A. Onuki, Europhys. Lett. **24**, 151 (1993). In applied shear flow, the velocity field around a droplet sensitively depends on the surface density ρ_s of adsorbed surfactant molecules. A crossover occurs for $\rho_s \sim \text{const.}/R$.

[12] A. Onuki, accepted in J. Chem. Phys. ; cond-mat. arXiv:0902.1204. In the van der Waals model of binary mixtures, the coefficients γ_1 in Eq.(2.35) and $\mathcal{K}$ in Eq.(4.3) may be expressed in terms of the molecular parameters of the two components.

[13] M. Japas and J.M.H. Levelt Sengers, AIChE J, **35**, 705 (1989); J. M. H. Levelt Sengers, J. of Supercritical Fluids, **4**, 215 (1991).

[14] I. B. Petsche and P. G. Debenedetti, J. Phys. Chem. **95**, 386 (1991).

[15] M. A. Anisimov, E. E. Gorodetskii, V. D. Kulikov, and J. V. Sengers, Phys. Rev. E **51**, 1199 (1995).

[16] A. V. Plyasunov and E. L. Shock, J. of Supercritical Fluids **20**, 91 (2001).

[17] A.I. Abdulagatov, G.V. Stepanov, and I.M. Abdulagatov, High Temp. **3**, 408 (2007).

[18] R. Vochten and G. Petre, J. of Colloid lnterface Sci. **42**, 320 (1973).

[19] M. A. Azouni, C. Normand, and G. Pétré, J. of Colloid Interface Sci.**239**, 509 (2001).

[20] H. Kasumi, P.J. Sides, and J. L. Anderson, J. of Colloid and Interface Sci. **276**, 239 (2004).

[21] Y. Abe, Ann. N.Y. Acad. Sci. 1077: 650 (2006).

[22] R. Savino, N. di Francescantonioa, R. Fortezzab, and Y. Abe, Acta Astronautica **61**, 16 (2007).

[23] R. Savino, A. Cecere, and R. Di Paola, International Journal of Heat and Fluid Flow, (2009), to be published.

[24] D. Bedeaux, A.M. Albano, and P. Mazur, Physica A,**82**, 438 (1976); D. Bedeaux, Advances in Chemical Physics, **64**, 47 (1986).

[25] L.D. Landau and E.M. Lifshitz, *Fluid Mechanics* (Pergamon, 1959).

[26] A. Onuki, *Phase Transition Dynamics* (Cambridge University Press, Cambridge, 2002). See Appendix 10E for general expressions of vectors in terms of the spherical harmonic functions.

[27] In dilute mixtures the expansion with respect to the fugacity $f_2 = e^{\mu/T}$ is more convenient, since f_2 tends to zero as $c \to 0$ [12].

[28] Y.P. Pao, Phys. Fluids **14**, 306 (1971).

[29] Y. Sone and Y. Onishi, J. Phys. Soc. Jpn. **35**, 1773 (1973).

[30] G. Fang and C. A. Ward, Phys. Rev. E **59**, 417 (1999); ibid. **59**, 441(1999)

[31] B. Braun, Ch. Ikier, H. Klein and D. Woermann, Chem. Phys. Lett. **233**, 565 (1995).

[32] J. Straub, Exp. Therm. and Fluid Sci. **9**, 253 (1994).

[33] A. Onuki and R.A. Ferrell, Physica A **164**, 245 (1990); A. Onuki, Phys. Rev. E **76**, 061126 (2007).